International Journal of Mechanics and Materials in Design manuscript No.
(will be inserted by the editor)

Extension of the layer removal technique for the measurement of residual stresses in layered anisotropic cylinders

H.W. Carpenter · R.G. Reid · R. Paskaramoorthy

20 November 2013

Abstract An extension of the layer removal technique is presented that allows the residual stresses within multilayered anisotropic pipes of any wall thickness to be determined. The method inherently satisfies the self-equilibrium requirement and limits the effects of measurement errors to the region local to the error. The thickness of each layer that is removed need not be uniform and is entirely independent of the thickness of each ply of material. Four example problems are considered. The first three allow results to be compared between the present method and previous work. The fourth problem demonstrates the method on a thick walled anisotropic pipe built up of $+45°/-45°$ plies for which no solution was previously available.

Keywords Residual stress · Layer removal · Cylinders · Anisotropic

1 Introduction

Residual stresses are inherent stress distributions present in manufactured parts and usually result from the manufacturing process. These stresses can be associated with premature failure since they are additive to the applied loading. It thus becomes important to know the residual stresses within a structure, especially where a conservative safety factor is impractical. Although considerable work has been done on the prediction of residual stresses, experimental measurement is often the most practical approach. The measurement of residual stresses can be divided into two techniques, namely non-destructive, and destructive. The two primary non-destructive methods of residual stress measurement are x-ray diffraction [1] and neutron diffraction [2]. Both of these methods have the disadvantage that they can only be used on crystalline materials [3] (and are consequently of no use for important materials such as glass fibre reinforced plastics) and they require specialised equipment, which is not readily accessible. As a consequence, destructive measurement techniques are

H.W. Carpenter · R.G. Reid (✉) · R. Paskaramoorthy
DST/NRF Centre of Excellence in Strong Materials and RP/Composites Facility
School of Mechanical, Industrial and Aeronautical Engineering
University of the Witwatersrand, Johannesburg
Private Bag 3, Wits, 2050, South Africa
E-mail: robert.reid@wits.ac.za

extensively used. A great variety have been developed, of which the most widely used include the layer removal method [4,5], crack compliance or slitting method [3,6,7], contour method [8,9], hole drilling method [10,11] and Sachs' method [12,13].

In composite materials, the major sources of residual stress are the cure shrinkage of the resin system, differences in the thermal and mechanical properties of the fibre and resin systems, and those of the different plies resulting from changes in material and/or fibre orientations. Most of the different destructive measurement techniques have been applied to the measurement of residual stresses in layered composite materials. Shokrieh et al. [14] used the crack compliance method to compare residual stresses in layered quasi-isotropic and cross-ply carbon/epoxy laminates with those calculated using the classical lamination theory. Ersoy and Vardar [15] compared the residual stress distribution in a $(0_{10}/90_{10})_s$ laminate using the crack compliance and layer removal methods. Bateman et al. [16] utilised finite element analysis to obtain the coefficients used to calculate the residual stress distribution in a carbon/epoxy plate based on hole distortions. Seif et al. [17,18] determined the residual stress distribution in thin-walled composite cylinders using a slitting type technique combined with an optical displacement measurement. Kim and Lee [19] measured the residual hoop stress in thick-walled carbon fibre pre-preg cylinders using what they described as the radial cut cylinder bending method. This method consists of splitting the pipe with a radial cut down its length, and measuring changes in strain on the inner and outer surfaces of the pipe due to the release of the residual bending moment. The residual stress was calculated using curved beam theory. Akbari et al. [20] utilised the crack compliance method, using pulse functions and Thikhonov regularization to obtain the residual hoop stress distribution in a layered carbon fibre ring. Chen et al. [21] utilised a layer removal and inherent strain technique to determine the residual stresses in layered isotropic tubes. They compared the results they obtained to those of Sachs' method.

The method developed by Sachs [12] relies on boring out the inner surface or removing the outer surface layers of a cylindrical pipe, and so can be considered a layer removal method. As originally developed, this approach is limited to isotropic materials. The approach has the advantage that the axial, circumferential, in-plane shear and radial residual stresses can be found. The method has seen use on both isotropic materials [22,23,13] and cylindrically orthotropic materials. The first work applied to the latter materials was presented by Olson and Bert [24] who modified Sachs' method to enable the residual stress distribution in cylindrically orthotropic bars and tubes to be determined. Voyiadjis et al. [25] presented a similar method for measuring residual stress in cylindrically orthotropic materials. Voyiadjis et al. [26] later presented an extended method of this work to obtain residual stresses in layered cylindrically orthotropic materials. Rasty et al. [27] utilised the method presented by Voyiadjis et al. [25], with a different derivation of the radial and hoop stresses, to obtain the residual stress distribution present in nuclear-grade zircaloy-4(R) tubes.

All of the methods presented by Olson et al. [24], Voyiadjis et al. [25,26], and Rasty et al. [27], are limited to orthotropic cylinders and cannot be applied to anisotropic cylinders. Additionally, they all determine the radial and hoop stresses arising from radial pressure by using the plane stress solution of Lekhnitskii [28] for annular plates. The use of the plane stress assumption is not, however, entirely correct for cylinders. The correct boundary condition is that the axial strain is invariant in the radial direction [29]. This permits self-equilibrating axial stresses to arise from the application of radial pressure loads. Although these stresses do not materialize in isotropic cylinders they become increasingly significant in orthotropic and anisotropic cylinders as the wall thickens. For this reason, the methods of Olson et al. [24], Voyiadjis et al. [25,26], and Rasty et al. [27] are limited to comparatively thin-walled orthotropic pipes.

The current paper presents an alternative approach that does not suffer from these constraints. It is based on the exact elastic solution for laminated anisotropic cylinders and correctly models the boundary conditions. As a consequence the technique is not limited in its use. In its full ramifications this allows the analysis of thick-walled, multilayered, anisotropic cylinders. To the authors' knowledge, no technique with this capability has been published before.

2 Theory

Basis of analysis

The present method of calculating the residual stresses in layered anisotropic pipes is based on the exact elastic solution for laminated cylindrical components presented in the excellent textbook of Herakovich [29]. This work is based upon those of Lekhnitskii [30], Scherrer [31], Reissner [32], Pagano [33], Reissner and Tsia [34] and Wilson and Orgill [35]. The laminated pipe under consideration is illustrated in Fig. 1.

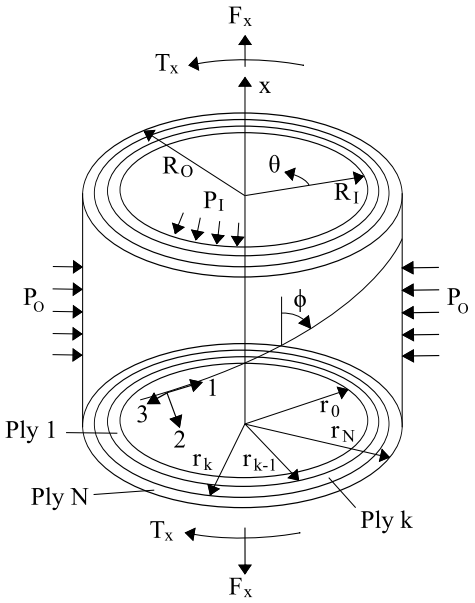

Fig. 1 Laminated composite pipe

Throughout this text, the term "ply" is reserved for a single lamina within the pipe laminate, whereas the term "layer" is reserved for material that is removed from the laminate during the experimental process. Measurement of the residual stresses within a ply typically requires its progressive removal in several layers.

For an orthotropic ply, the elastic constitutive equations in the material coordinate system [29] are

$$\begin{bmatrix} \sigma_1 \\ \sigma_2 \\ \sigma_3 \\ \tau_{23} \\ \tau_{31} \\ \tau_{12} \end{bmatrix} = \begin{bmatrix} C_{11} & C_{12} & C_{13} & 0 & 0 & 0 \\ C_{12} & C_{22} & C_{23} & 0 & 0 & 0 \\ C_{13} & C_{23} & C_{33} & 0 & 0 & 0 \\ 0 & 0 & 0 & C_{44} & 0 & 0 \\ 0 & 0 & 0 & 0 & C_{55} & 0 \\ 0 & 0 & 0 & 0 & 0 & C_{66} \end{bmatrix} \begin{bmatrix} \varepsilon_1 \\ \varepsilon_2 \\ \varepsilon_3 \\ \gamma_{23} \\ \gamma_{31} \\ \gamma_{12} \end{bmatrix} \tag{1}$$

For an orthotropic ply at a fibre angle ϕ measured from the axial orientation, the elastic constitutive equations of Eq. (1) are transformed into those of a monoclinic material in the cylindrical coordinate system (r,θ,x) [29]:

$$\begin{bmatrix} \sigma_x \\ \sigma_\theta \\ \sigma_r \\ \tau_{\theta r} \\ \tau_{xr} \\ \tau_{x\theta} \end{bmatrix} = \begin{bmatrix} \bar{C}_{11} & \bar{C}_{12} & \bar{C}_{13} & 0 & 0 & \bar{C}_{16} \\ \bar{C}_{12} & \bar{C}_{22} & \bar{C}_{23} & 0 & 0 & \bar{C}_{26} \\ \bar{C}_{13} & \bar{C}_{23} & \bar{C}_{33} & 0 & 0 & \bar{C}_{36} \\ 0 & 0 & 0 & \bar{C}_{44} & \bar{C}_{45} & 0 \\ 0 & 0 & 0 & \bar{C}_{45} & \bar{C}_{55} & 0 \\ \bar{C}_{16} & \bar{C}_{26} & \bar{C}_{36} & 0 & 0 & \bar{C}_{66} \end{bmatrix} \begin{bmatrix} \varepsilon_x \\ \varepsilon_\theta \\ \varepsilon_r \\ \gamma_{\theta r} \\ \gamma_{xr} \\ \gamma_{x\theta} \end{bmatrix} \tag{2}$$

The inter-laminar shear stresses $\tau_{\theta r}$ and τ_{xr} can be written as

$$\tau_{\theta r} = \frac{B}{r^2} \tag{3}$$

$$\tau_{xr} = \frac{C}{r} \tag{4}$$

where B and C are constants of integration [29]. Traction continuity between layers requires the inter-laminar shear stresses $\tau_{\theta r}$ and τ_{xr} to be continuous from layer to layer. Since these shear stresses must be zero at the inner and outer surfaces of the pipe, B and C are consequently zero [29]. Thus, Eq. (2) reduces to

$$\begin{bmatrix} \sigma_x \\ \sigma_\theta \\ \sigma_r \\ \tau_{x\theta} \end{bmatrix} = \begin{bmatrix} \bar{C}_{11} & \bar{C}_{12} & \bar{C}_{13} & \bar{C}_{16} \\ \bar{C}_{12} & \bar{C}_{22} & \bar{C}_{23} & \bar{C}_{26} \\ \bar{C}_{13} & \bar{C}_{23} & \bar{C}_{33} & \bar{C}_{36} \\ \bar{C}_{16} & \bar{C}_{26} & \bar{C}_{36} & \bar{C}_{66} \end{bmatrix} \begin{bmatrix} \varepsilon_x \\ \varepsilon_\theta \\ \varepsilon_r \\ \gamma_{x\theta} \end{bmatrix} \tag{5}$$

At positions remote from edge effects, the displacements in the axial (u), tangential (v) and radial (w) directions, at the radial position r and axial position x for the k^{th} ply of an anisotropic pipe can be written [29] as

$$u^k(x,r) = \varepsilon_x^0 x \tag{6}$$

$$v^k(x,r) = \gamma^0 xr \tag{7}$$

$$w^k(r) = A_1^k r^{\lambda^k} + A_2^k r^{-\lambda^k} + \Gamma^k \varepsilon_x^0 r + \Omega^k \gamma^0 r^2 \tag{8}$$

where ε_x^0, γ^0, A_1^k and A_2^k are constants determined by the specified boundary and loading conditions. The terms λ^k, Γ^k and Ω^k are constant terms dependent on the material properties of the k^{th} ply [29]:

$$\lambda^k = \sqrt{\frac{\bar{C}_{22}^k}{\bar{C}_{33}^k}} \tag{9}$$

$$\Gamma^k = \frac{\bar{C}_{12}^k - \bar{C}_{13}^k}{\bar{C}_{33}^k - \bar{C}_{22}^k} \tag{10}$$

$$\Omega^k = \frac{\bar{C}_{26}^k - 2\bar{C}_{36}^k}{4\bar{C}_{33}^k - \bar{C}_{22}^k} \tag{11}$$

Individual ply strains at the radial position r for the k^{th} ply can be written [29] as

$$\varepsilon_x^k = \varepsilon_x^0 \tag{12}$$

$$\varepsilon_\theta^k = A_1^k r^{\left(\lambda^k - 1\right)} + A_2^k r^{\left(-\lambda^k - 1\right)} + \Gamma^k \varepsilon_x^0 + \Omega^k \gamma^0 r \tag{13}$$

$$\varepsilon_r^k = \lambda^k A_1^k r^{\left(\lambda^k - 1\right)} - \lambda^k A_2^k r^{\left(-\lambda^k - 1\right)} + \Gamma^k \varepsilon_x^0 + 2\Omega^k \gamma^0 r \tag{14}$$

$$\gamma_{x\theta}^k = \gamma^0 r \tag{15}$$

The stresses in each ply are determined using Eqs. (16) to (19) [29]:

$$\begin{aligned}\sigma_x^k = &\left[\bar{C}_{11}^k + \left(\bar{C}_{13}^k + \bar{C}_{12}^k\right)\Gamma^k\right]\varepsilon_x^0 + \left[\left(\bar{C}_{12}^k + 2\bar{C}_{13}^k\right)\Omega^k + \bar{C}_{16}^k\right]\gamma^0 r \\ &+ \left[\bar{C}_{12}^k + \lambda^k \bar{C}_{13}^k\right] A_1^k r^{\left(\lambda^k - 1\right)} + \left[\bar{C}_{12}^k - \lambda^k \bar{C}_{13}^k\right] A_2^k r^{\left(-\lambda^k - 1\right)}\end{aligned} \tag{16}$$

$$\begin{aligned}\sigma_\theta^k = &\left[\bar{C}_{12}^k + \left(\bar{C}_{22}^k + \bar{C}_{23}^k\right)\Gamma^k\right]\varepsilon_x^0 + \left[\left(\bar{C}_{22}^k + 2\bar{C}_{23}^k\right)\Omega^k + \bar{C}_{26}^k\right]\gamma^0 r \\ &+ \left[\bar{C}_{22}^k + \lambda^k \bar{C}_{23}^k\right] A_1^k r^{\left(\lambda^k - 1\right)} + \left[\bar{C}_{22}^k - \lambda^k \bar{C}_{23}^k\right] A_2^k r^{\left(-\lambda^k - 1\right)}\end{aligned} \tag{17}$$

$$\begin{aligned}\sigma_r^k = &\left[\bar{C}_{13}^k + \left(\bar{C}_{23}^k + \bar{C}_{33}^k\right)\Gamma^k\right]\varepsilon_x^0 + \left[\left(\bar{C}_{23}^k + 2\bar{C}_{33}^k\right)\Omega^k + \bar{C}_{36}^k\right]\gamma^0 r \\ &+ \left[\bar{C}_{23}^k + \lambda^k \bar{C}_{33}^k\right] A_1^k r^{\left(\lambda^k - 1\right)} + \left[\bar{C}_{23}^k - \lambda^k \bar{C}_{33}^k\right] A_2^k r^{\left(-\lambda^k - 1\right)}\end{aligned} \tag{18}$$

$$\begin{aligned}\tau_{x\theta}^k = &\left[\bar{C}_{16}^k + \left(\bar{C}_{26}^k + \bar{C}_{36}^k\right)\Gamma^k\right]\varepsilon_x^0 + \left[\bar{C}_{66}^k + \left(\bar{C}_{26}^k + 2\bar{C}_{36}^k\right)\Omega^k\right]\gamma^0 r \\ &+ \left[\bar{C}_{26}^k + \lambda^k \bar{C}_{36}^k\right] A_1^k r^{\left(\lambda^k - 1\right)} + \left[\bar{C}_{26}^k - \lambda^k \bar{C}_{36}^k\right] A_2^k r^{\left(-\lambda^k - 1\right)}\end{aligned} \tag{19}$$

For perfectly bonded layers, all displacements must be continuous from layer to layer, as must the radial stress at each ply interface. The radial stress at the inner and outer walls of the pipe is exactly equal and opposite to the pressure applied on the respective surfaces. These requirements are formulated in Eqs. (20) to (25) [29] and are used to obtain the constants ε_x^0 and γ^0 and the ply constants A_1^k and A_2^k [29].

$$\varepsilon^{0^k} = \varepsilon_x^0 \quad (k = 1, \ldots, N) \tag{20}$$

$$\gamma^{0^k} = \gamma^0 \quad (k = 1, \ldots, N) \tag{21}$$

$$w^k = w^{k+1} \quad (\text{Interface at } r_k \; k = 1, \ldots, N-1) \tag{22}$$

$$\sigma_r^k = \sigma_r^{k+1} \quad (\text{Interface at } r_k \; k = 1, \ldots, N-1) \tag{23}$$

$$\sigma_r(R_I) = -P_I \tag{24}$$

$$\sigma_r(R_O) = -P_O \tag{25}$$

In the above, P_I and P_O indicate the pressures acting on the inner and outer surfaces, respectively.

2.1 Obtaining residual stresses

The residual stress distribution is determined by progressively releasing stress through the removal of material, and measuring the associated changes in strain elsewhere in the pipe. It is assumed in this work that the removal of material progresses inwards from the outside of the pipe and that the strain is measured on the inner surface. Removal of material in the reverse direction can, however, easily be accommodated. The assumption is made that the elimination of a layer of material from the outer surface of the pipe causes a purely elastic mechanical response in the remaining pipe section. Practically, this means that care must be taken to ensure that machining loads and heating are minimised.

Strain gauge rosettes are required so that the axial strain ε_x, hoop strain ε_θ and in-plane shear strain $\gamma_{x\theta}$ responses can be determined. Since the constants ε_x^0 and γ^0 that arise in the response to the release of residual stress in the removed layer are invariant throughout the wall thickness, $\varepsilon_x = \varepsilon_x^0$ and $\gamma_{x\theta} = \gamma^0$. The measured strains after the removal of m layers allow the calculation of the cumulative residual load that has been released. This load can be modelled as an axial force and torque applied to the remaining pipe of N plies, as well as an external pressure applied at the newly exposed outer surface. The requirement is that the application of these loads must result in the same strains that are measured after the removal of all m layers of material from the outside of the pipe. It should be noted that the thickness of each layer removed need not be uniform and is entirely independent of the thickness of each ply.

Prior to the calculation of the loads applied to the remaining pipe thickness, the constants A_1^k and A_2^k for each ply in the remaining pipe section are determined. The number of plies remaining is equal to N which means that N constants A_1^k and N constants A_2^k must be determined, or $2N$ unknowns in total. This is done by utilising Eq. (18) where the radial stress at the inner surface of the pipe is always zero, and Eq. (13) where the measured strain is analytically expressed in relation to the required constants. Additionally, the $2(N-1)$ equilibrium conditions are simultaneously applied in the form of Eqs. (22) and (23) at each ply interface, which requires the use of Eqs. (8) and (18). The equations resulting from this approach are written in matrix form:

$$\boldsymbol{DA} = \boldsymbol{M} \tag{26}$$

The non-zero terms of the square matrix $\boldsymbol{D}$ are determined as

$$\left.\begin{aligned} D_{1,1} &= \beta^1 r_0^{(\lambda^1-1)} \\ D_{1,2} &= \delta^1 r_0^{(-\lambda^1-1)} \\ D_{2,1} &= r_0^{(\lambda^1-1)} \\ D_{2,2} &= r_0^{(-\lambda^1-1)} \end{aligned}\right\} \text{For } k=1 \tag{27}$$

$$\left.\begin{aligned} D_{2k+1,2k-1} &= \beta^k r_k^{(\lambda^k-1)} \\ D_{2k+1,2k} &= \delta^k r_k^{(-\lambda^k-1)} \\ D_{2k+1,2k+1} &= -\beta^{k+1} r_k^{(\lambda^{k+1}-1)} \\ D_{2k+1,2k+2} &= -\delta^{k+1} r_k^{(-\lambda^{k+1}-1)} \\ D_{2k+2,2k-1} &= r_k^{\lambda^k} \\ D_{2k+2,2k} &= r_k^{-\lambda^k} \\ D_{2k+2,2k+1} &= -r_k^{\lambda^{k+1}} \\ D_{2k+2,2k+2} &= -r_k^{-\lambda^{k+1}} \end{aligned}\right\} \text{For } 1 \le k \le N-1 \tag{28}$$

where

$$\beta^k = \bar{C}_{23}^k + \lambda^k \bar{C}_{33}^k \tag{29}$$

and

$$\delta^k = \bar{C}_{23}^k - \lambda^k \bar{C}_{33}^k \tag{30}$$

Eq. (27) relates to the boundary conditions on the inner surface, while Eq. (28) relates to the boundary conditions of continuous radial stress and radial displacement at each ply interface. Equation (28) is only applicable when the number of plies remaining in the pipe is greater than one.
The terms of vector $\boldsymbol{A}$ in Eq. (26) are

$$\left.\begin{aligned} A_{2k-1} &= A_1^k \\ A_{2k} &= A_2^k \end{aligned}\right\} \text{For } 1 \le k \le N \tag{31}$$

The vector $\boldsymbol{M}$ in Eq. (26) is expressed in terms of the measured strain ε_θ and constant strain

terms ε_x^0 and γ^0.

$$\left.\begin{array}{l} M_1 = -\eta^1 \varepsilon_x^0 - \kappa^1 \gamma^0 r_0 \\ M_2 = \varepsilon_\theta - \Gamma^1 \varepsilon_x^0 - \Omega^1 \gamma^0 r_0 \end{array}\right\} \text{For } k = 1 \tag{32}$$

$$\left.\begin{array}{l} M_{2k+1} = -\eta^k \varepsilon_x^0 - \kappa^k \gamma^0 r_k \\ \qquad\quad +\eta^{k+1} \varepsilon_x^0 + \kappa^{k+1} \gamma^0 r_k \\ M_{2k+2} = -\Gamma^k \varepsilon_x^0 r_k - \Omega^k \gamma^0 r_k^2 \\ \qquad\quad +\Gamma^{k+1} \varepsilon_x^0 r_k + \Omega^{k+1} \gamma^0 r_k^2 \end{array}\right\} \text{For } 1 \le k \le N-1 \tag{33}$$

where

$$\eta^k = \bar{C}_{13}^k + \left[\bar{C}_{23}^k + \bar{C}_{33}^k\right] \Gamma^k \tag{34}$$

and

$$\kappa^k = \left[\bar{C}_{23}^k + 2\bar{C}_{33}^k\right] \Omega^k + \bar{C}_{36}^k \tag{35}$$

As with Eq. (28), Eq. (33) is only applicable to a pipe where the remaining number of plies is greater than one.

Once the constants A_1^k and A_2^k in each of the plies of the remaining pipe section are found by solving Eq. (26), the internal stresses and the pressure applied to the outer surface can be found using Eqs. (16) to (19) while invoking Eq. (25). These stresses result from the removal of the outer m layers of pipe section and are modelled as externally applied loads acting in the remaining pipe thickness. The axial force, F_x, and torque, T_x, existing at the ends of the remaining pipe of N plies are shown in Eqs. (36) and (37) respectively.

$$\begin{aligned} F_x &= \int_{r_0}^{r_N} 2\pi \sigma_x r \, dr \\ &= 2\pi \sum_{k=1}^{N} \int_{r_{k-1}}^{r_k} \sigma_x^k r \, dr \\ &= 2\pi \sum_{k=1}^{N} \left[\left(\bar{C}_{11}^k + \left\{ \bar{C}_{13}^k + \bar{C}_{12}^k \right\} \Gamma^k \right) \varepsilon_x^0 \left(\frac{r_k^2 - r_{k-1}^2}{2} \right) \right. \\ &\quad + \left(\bar{C}_{16}^k + \left\{ \bar{C}_{12}^k + 2\bar{C}_{13}^k \right\} \Omega^k \right) \gamma^0 \left(\frac{r_k^3 - r_{k-1}^3}{3} \right) \\ &\quad + \frac{\left(\bar{C}_{12}^k + \lambda^k \bar{C}_{13}^k\right)}{\lambda^k + 1} A_1^k \left(r_k^{(\lambda^k+1)} - r_{k-1}^{(\lambda^k+1)} \right) \\ &\quad \left. + \frac{\left(\bar{C}_{12}^k - \lambda^k \bar{C}_{13}^k\right)}{-\lambda^k + 1} A_2^k \left(r_k^{(-\lambda^k+1)} - r_{k-1}^{(-\lambda^k+1)} \right) \right] \end{aligned} \tag{36}$$

$$
\begin{aligned}
T_x =& 2\pi \int_{r_0}^{r_N} \tau_{x\theta} r^2 \, dr \\
=& 2\pi \sum_{k=1}^{N} \left[\left(\bar{C}_{16}^k + \left\{ \bar{C}_{26}^k + \bar{C}_{36}^k \right\} \Gamma^k \right) \varepsilon_x^0 \left(\frac{r_k^3 - r_{k-1}^3}{3} \right) \right. \\
&+ \left(\bar{C}_{66}^k + \left\{ \bar{C}_{26}^k + 2\bar{C}_{36}^k \right\} \Omega^k \right) \gamma^0 \left(\frac{r_k^4 - r_{k-1}^4}{4} \right) \\
&+ \frac{\left(\bar{C}_{26}^k + \lambda^k \bar{C}_{36}^k \right)}{\lambda^k + 2} A_1^k \left(r_k^{\left(\lambda^k+2\right)} - r_{k-1}^{\left(\lambda^k+2\right)} \right) \\
&\left. + \frac{\left(\bar{C}_{26}^k - \lambda^k \bar{C}_{36}^k \right)}{-\lambda^k + 2} A_2^k \left(r_k^{\left(-\lambda^k+2\right)} - r_{k-1}^{\left(-\lambda^k+2\right)} \right) \right]
\end{aligned} \tag{37}
$$

The loads released by each individual layer, $F_x^{\bar{m}}$ and $T_x^{\bar{m}}$, are found by subtracting the loads that exist after $m-1$ layers are removed from those that exist after m layers are removed.

$$
F_x^{\bar{m}} = \begin{cases} F_x^m & (\text{for } m = 1) \\ F_x^m - F_x^{m-1} & (\text{for } m > 1) \end{cases} \tag{38}
$$

$$
T_x^{\bar{m}} = \begin{cases} T_x^m & (\text{for } m = 1) \\ T_x^m - T_x^{m-1} & (\text{for } m > 1) \end{cases} \tag{39}
$$

The applied pressure, P_O^m, is found by using Eqs. (18) and (25). After the removal of m layers, the resultant radial stress at the surface is the sum of the radial residual stress that existed prior to the removal of the outer layers and the calculated radial stress that arises due to the removal of these layers. Since the resultant radial stress at the outer surface of the remaining pipe must vanish, the residual radial stress is equal the negative of the radial stress calculated using Eq. (18). The applied pressure, P_O^m, is therefore exactly equal to the residual radial stress. It is apparent from Eqs. (38) and (39) that the loads calculated for layer m are affected only by those calculated for the removal of layers m and $m-1$. This indicates that errors in stress arising from measurement inaccuracies do not propagate beyond the layer following on from the erroneous reading.

The stress distributions within the newly removed layer m, which are determined using Eqs. (16) to (19), require knowledge of the four constants A_1, A_2, ε_x^0 and γ^0 within this layer. These unknowns are found making use of the four boundary conditions arising from the application of the axial and torsional loads, $F_x^{\bar{m}}$ and $T_x^{\bar{m}}$, and the known radial residual stresses that were obtained for the inner and outer surfaces of this layer. If the removed layer contains an interface between two different materials, the appropriate boundary conditions of Eqs. (22) and (23) must be included into the solution.

Accuracy considerations

Residual stresses in the hoop and axial directions must have a zero force resultant. Due to the cylindrical nature of the problem, a zero moment state is not required. The overall torque

must, however, have a zero resultant. The present analysis assumes that the loads applied to the remaining pipe section arise from the release of residual stresses and that no external loads are applied. F_x^m and T_x^m must therefore tend to zero as m increases and the pipe tends to zero wall thickness. Since these loads represent the loads applied to the remaining section by the removal of the outer layers, the resultant force of the calculated stress distribution must therefore tend towards zero. This method therefore generates stress distributions that satisfy the self-equilibrium requirement. Additionally, since F_x^m and T_x^m are defined for the removal of m plies, and the individual layer loads calculated using Eqs. (38) and (39) are based only on the values of F_x^m, F_x^{m-1}, T_x^m and T_x^{m-1} respectively, errors do not propagate through the thickness of the pipe wall. An error in F_x^m will cause a corresponding error in the stress arising from $F_x^{\bar{m}}$. If the value of F_x^{m+1} is accurate, an opposing error in $F_x^{\bar{m}+1}$ (and its resultant stress) is required as a consequence of there being no external loading. This error does not, however, propagate to the $(m+2)$ layer. There thus exists a built-in system of self-correction. The same can be said for T_x^m.

Since the analysis approach is based on an exact elastic solution, the coupling between the stress components is properly considered. This means that the technique is not limited to any particular class of problem. It can be applied to any combination of material type, wall thickness and lamination sequence. The stress distributions within a multi-layered, thick-walled, anisotropic pipe can consequently be accurately determined, as can those of any simpler configuration.

3 Results and discussion

To illustrate the accuracy and capabilities of the method, four example problems of increasing complexity are considered. The simplest problem is that of a thick-walled isotropic pipe, the thin-walled case being trivial. Thin and thick-walled orthotropic pipes are then considered followed by a layered thick-walled anisotropic pipe.

3.1 Problem 1: Thick-walled isotropic pipe

The pipe under consideration is assumed to have inner diameter of 80 mm and wall thickness of 150 mm. This corresponds to a wall-thickness to inner-diameter ratio (t/d_i) of 1.875. The material properties are those of steel, E = 200 GPa and ν = 0.3. It is assumed that material is removed from the outer surface of the pipe and the strain response is measured on the inner surface. The objective then becomes to determine the residual stress distribution, given the variations in measured strain with removed material. For the purpose of this exercise, all three components of the measured strain response are assumed to vary linearly as presented in Fig. 2. It should be noted, however, that the method is applicable for any variation in measured strain.

The removal of material from the outer diameter of the pipe causes a strain response in the remaining material. The three strain components presented in Fig. 2 are directly measured on the inner wall. This problem only has a single material type and so only the two constants A_1^1 and A_2^1 are required. These are found using Eq. (26) which requires knowledge of the measured strains and the material properties. Once the constants A_1^1 and A_2^1 are known, they are used with the constant strains, ε_x^0 and γ^0, to determine the axial load, torque and external pressure applied to the remaining pipe thickness by the removed material. These loads are directly calculated using Eqs. (36), (37) and (18), respectively. If a further thin layer of

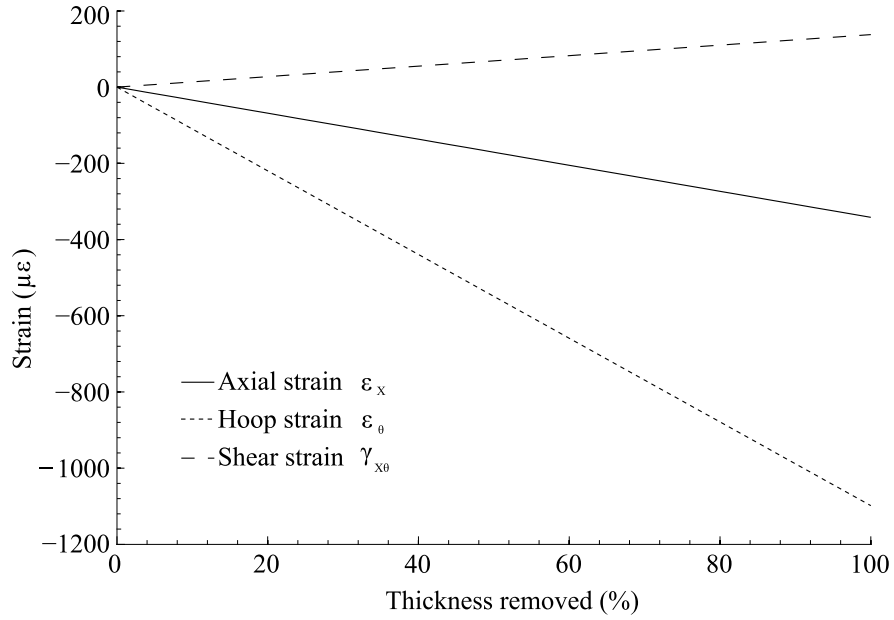

Fig. 2 Assumed linear distribution of strain measurements

material is removed from the outer diameter of the pipe, the measured values of the strain response change, and so new constants A_1^1 and A_2^1 in the smaller pipe are determined. The loads applied by all the removed material to the slightly smaller pipe are then found. The loads that originally existed in the newly removed material must be equal to the difference in the loads applied to these two pipes. The differences between the axial and torque loads are consequently applied to a thin walled pipe corresponding to the removed layer. Additionally, the negative of the pressure loads acting on the larger and smaller diameter pipes are applied on the outer and inner surfaces, respectively. The boundary conditions resulting from the applied axial load, the applied torque and the pressure loads on the inner and outer surfaces allow the calculation of the constants ε_x^0, γ^0, A_1^1 and A_2^1 in the newly removed layer. Eqs. (36) and (37) and two applications of Eq. (18), one each for the pressures on the inner and outer surfaces, respectively, are used. Once the constants in the newly removed layer are known, the stress distributions within this layer are found using Eqs. (16) to (19).

Results obtained using this technique are compared against those of Sachs [12], Voyiadjis et al. [25] and Rasty et al. [27]. The axial, σ_x, and hoop, σ_θ, residual stress distributions are presented in Figs. 3 and 4, respectively. The radial, σ_r, and in-plane shear stress, $\tau_{x\theta}$, distributions are shown in Fig. 5. It is clear that the results obtained by the present method, that of Voyiadjis et al. [25] and that of Sachs [12] are indistinguishable within the resolution of the figures. The hoop residual stress obtained using the method of Rasty et al. [27], however, differs significantly from those of the other methods and is erroneous. Equilibrium considerations dictate that the integral of the hoop stress across the thickness must be equal to zero if no external pressure is applied and this is clearly not the case. The method of Rasty et al. [27] will consequently not be considered any further in this paper.

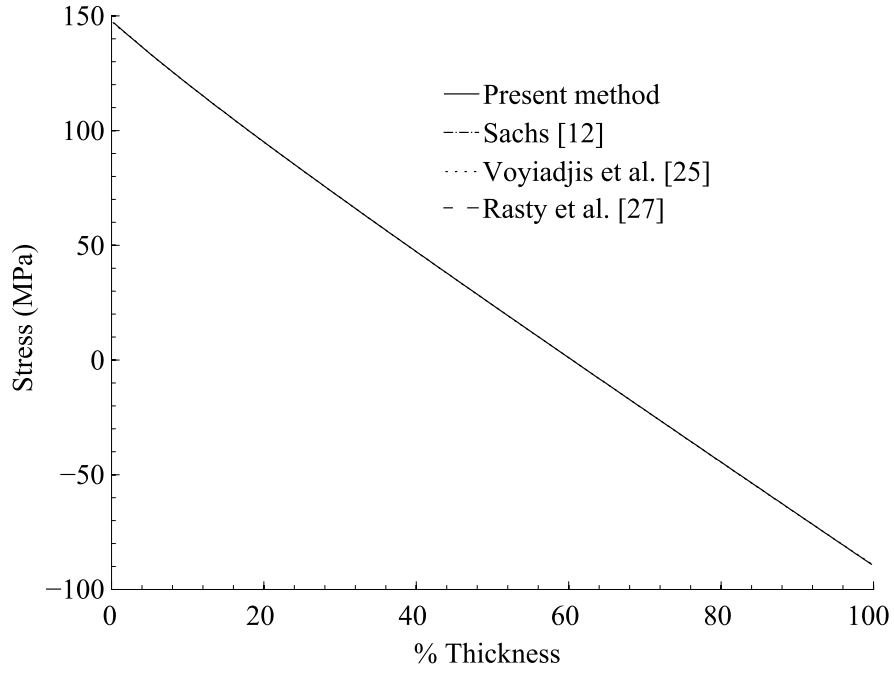

Fig. 3 Axial residual stress distribution for isotropic pipe, ($t/d_i = 1.875$)

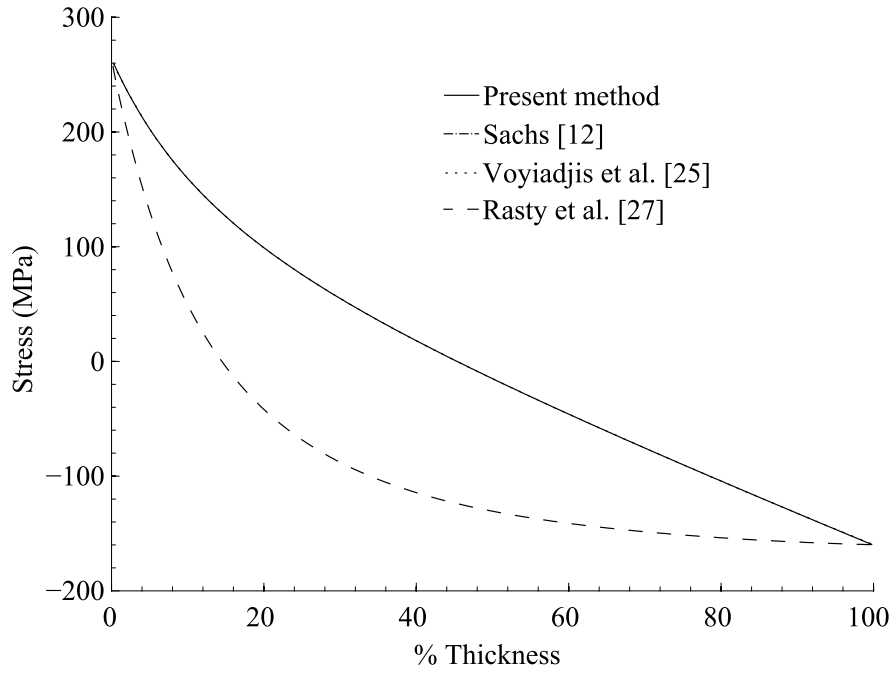

Fig. 4 Hoop residual stress distribution for isotropic pipe, ($t/d_i = 1.875$)

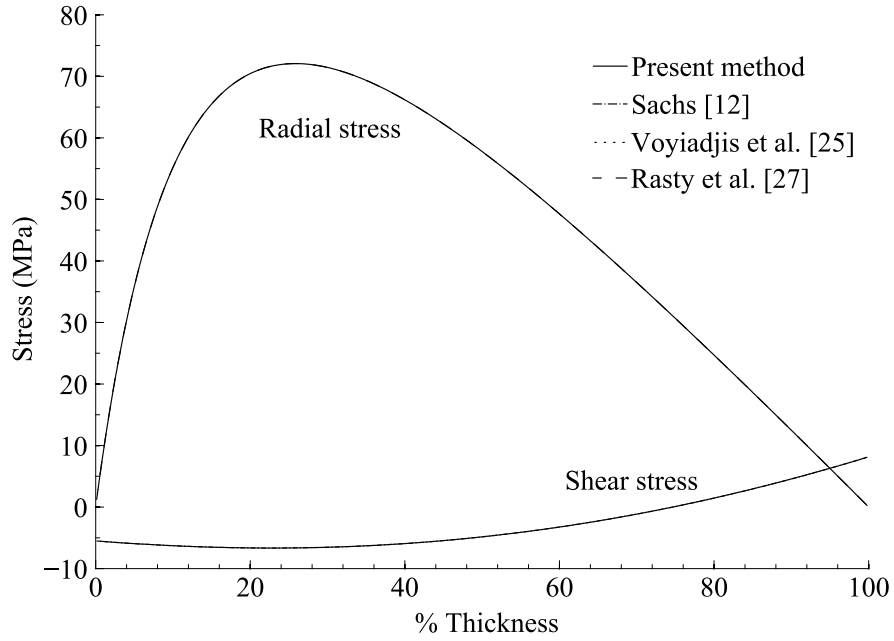

Fig. 5 Radial and in-plane shear stress distributions for isotropic pipe, ($t/d_i = 1.875$)

3.2 Problem 2: Thin-walled orthotropic pipe

This problem considers the case of an orthotropic pipe with an inner diameter of 80 mm and wall thickness of 1.5 mm, corresponding to t/d_i = 0.01875. The material properties are listed in Table 1. The measured strain distributions are the same as those of Problem 1.

Results obtained from the present method are compared with those of Voyiadjis et al. [25]. The axial, hoop, radial and shear residual stress distributions are shown in Figs. 6 and 7. As was the case for Problem 1, the results from the two methods are indistinguishable for all four stress components within the resolution of the figures.

Table 1 Material properties

Axial modulus, E_x (MPa)	6823
Hoop modulus, E_θ (MPa)	13730
Radial modulus, E_r (MPa)	8422
Shear modulus, $G_{x\theta}$ (MPa)	10186
Shear modulus, G_{xr} (MPa)	2718
Shear modulus, $G_{\theta r}$ (MPa)	2575
Poissons ratio, $\nu_{x\theta}$	0.445
Poissons ratio, ν_{xr}	0.280
Poissons ratio, $\nu_{\theta r}$	0.895

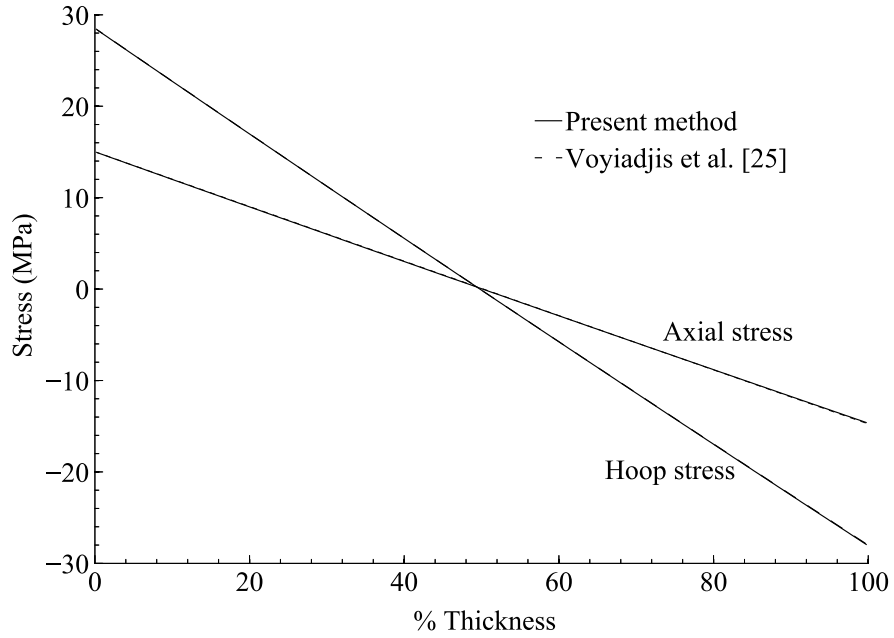

Fig. 6 Axial and hoop residual stress distributions for orthotropic pipe, ($t/d_i = 0.01875$)

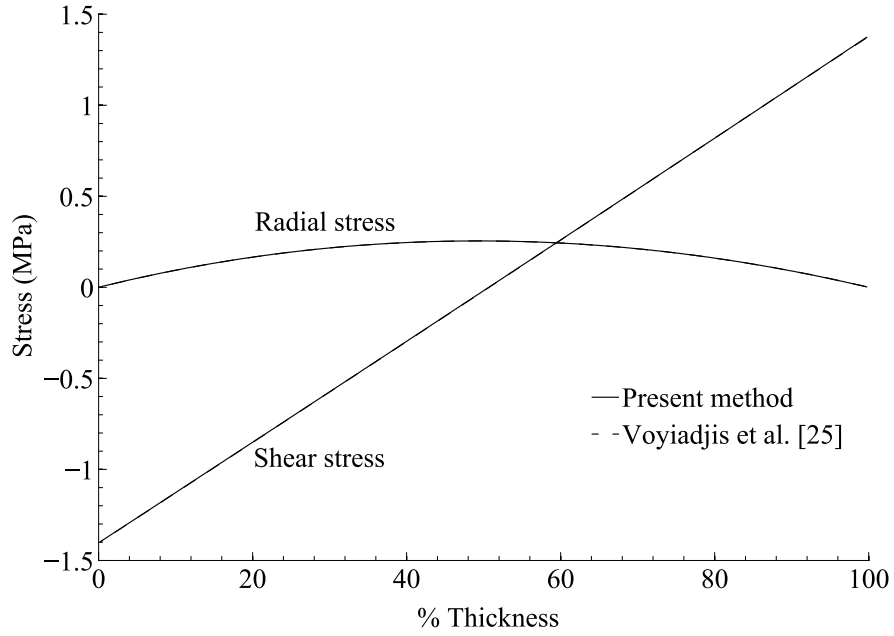

Fig. 7 Radial and in-plane shear stress distributions for orthotropic pipe, ($t/d_i = 0.01875$)

3.3 Problem 3: Thick-walled orthotropic pipe

An orthotropic pipe with an inner diameter of 80 mm and wall thickness of 150 mm, corresponding to t/d_i = 1.875, is considered. The material properties are the same as those of Problem 2 and the measured strain distributions are those of Problems 1 and 2.

The axial, σ_x, and hoop, σ_θ, residual stress distributions within the wall of this pipe are shown in Figs. 8 and 9, respectively. In contrast to the results for the thin-walled pipe, significant differences in the axial and hoop stresses are observed between the present method and that of Voyiadjis et al. [25]. It is not possible to identify any of the stress distributions as erroneous on the basis of self-equilibrium since they all satisfy this requirement. For this reason, a three-dimensional finite element analysis (FEA) was performed to determine the residual stress distribution through the wall-thickness.

The finite element analysis approached the problem in a similar way to the analytical technique. The residual stresses at a particular diameter were found by modelling two pipes. These pipes had remaining diameters slightly larger and slightly smaller than the diameter of interest. An axial force, a torque and an external pressure were individually applied to each of the two pipes. In the case of the force and torque, it was necessary to ensure that these loads were correctly distributed in the radial direction. This was achieved by constraining to zero the axial displacement and the circumferential angular displacement at one end of the pipe while constraining these parameters at the other end to be uniform. The boundary conditions of uniform axial strain and uniform in-plane shear strain of Eqs. (20) and (21) were thereby satisfied. The unique combination of axial load, torque and external pressure that resulted in the measured strains at each of the pipe diameters was calculated. A third pipe was then modelled, corresponding to the thin layer of material making up the difference in diameter between the first two models. The differences between the axial and torque loads required to obtain the measured strains of the first and second models was then applied to the third model. In addition, the negative of the pressure loads found for the larger and smaller diameter pipes were applied on the outer and inner surfaces, respectively. This loading generated the residual stress distribution within the thin layer of material around the diameter of interest, allowing each of the stress components to be determined. It is clear that the results obtained from this analysis agree extremely well with the axial and hoop stresses obtained using the present method and that the results of Voyiadjis et al. [25] are inaccurate for this thick-walled pipe.

Fig. 10 presents the radial, σ_r, and in-plane shear, $\tau_{x\theta}$, residual stress distributions in the pipe. Significant differences in the radial residual stresses calculated using the two methods are evident. This is somewhat expected since the radial and hoop stresses are related [25] via the relationship: $\sigma_\theta = \frac{\partial}{\partial r}(r\sigma_r)$. Since the hoop stress distribution calculated using the method of Voyiadjis et al. [25] is inaccurate, the radial stress distribution must also be in error. This is confirmed by the results of the FEA. Despite the differences in normal stresses, there is good agreement between the residual in-plane shear stresses predicted by the present method and that of Voyiadjis et al.. This is possible because there is no coupling between the normal strains and shear stresses in an orthotropic material.

3.4 Problem 4: Thick-walled, layered anisotropic pipe

The layered, anisotropic pipe under consideration has an inner diameter of 80 mm and wall thickness of 15 mm which corresponds to t/d_i = 0.1875. The wall thickness is built up of two layers of equal thickness. The fibres are aligned at $+45°$ and $-45°$ in the inner and outer

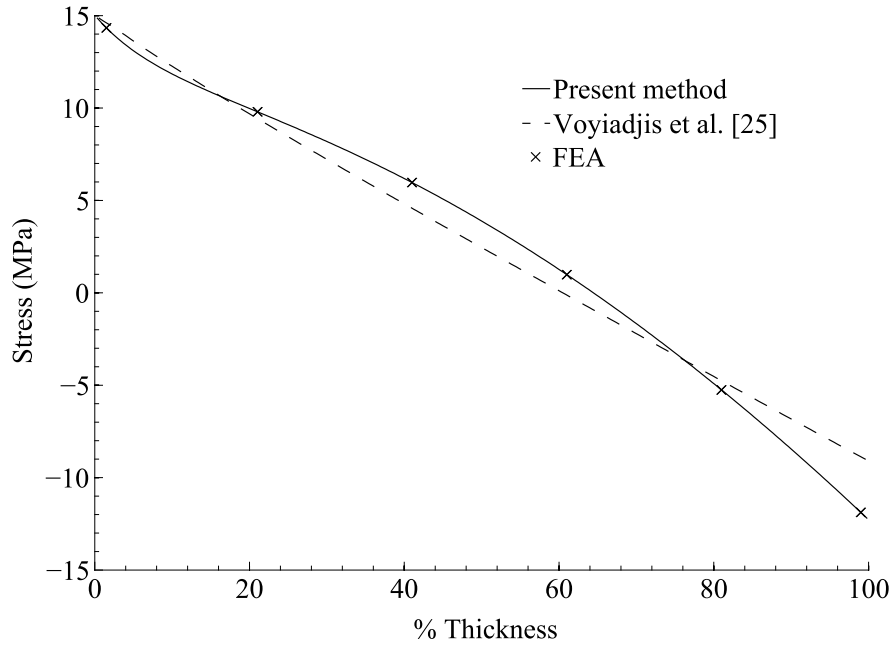

Fig. 8 Axial residual stress distribution for orthotropic pipe, ($t/d = 1.875$)

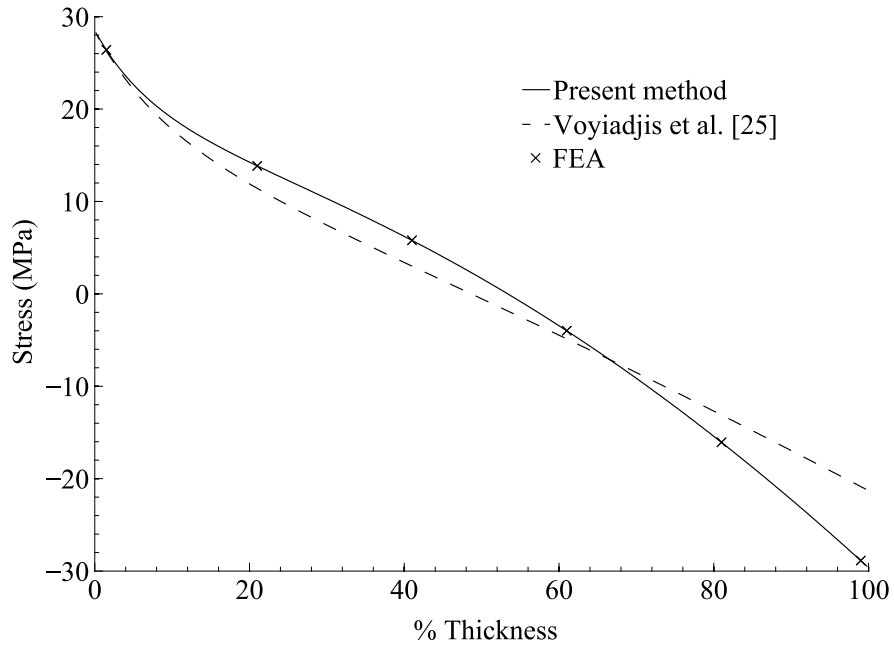

Fig. 9 Hoop residual stress distribution for orthotropic pipe, ($t/d = 1.875$)

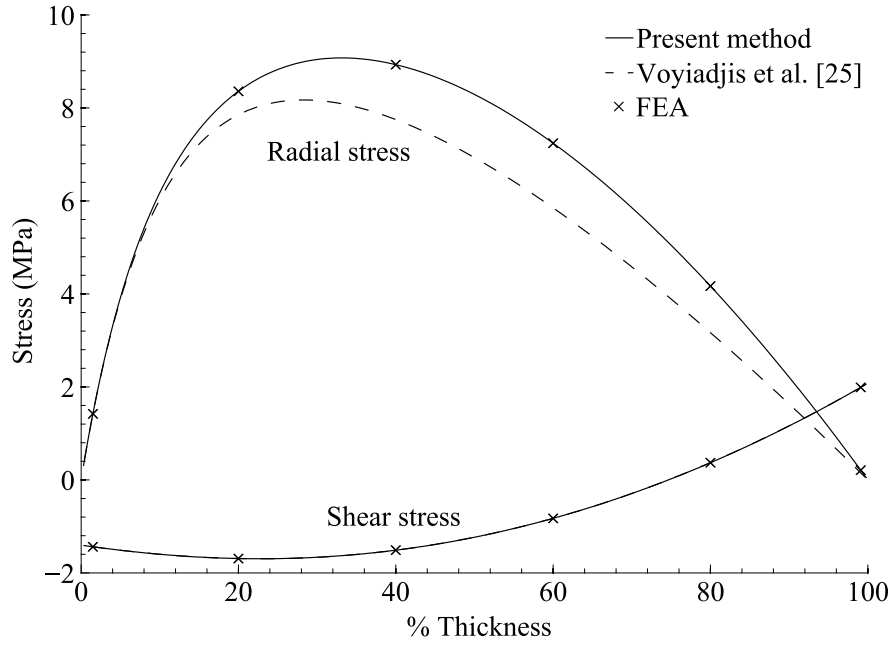

Fig. 10 Radial and in-plane shear stress distributions for orthotropic pipe, ($t/d = 1.875$)

layers, respectively. The material properties, in the material coordinate system, are presented in Table 2. It should be noted that this problem is chosen to illustrate the power of the present method and that the method of Voyiadjis et al. [25] is invalid in this case. The problem is solved in the same manner as the three previous problems except that the presence of the additional layer requires that two extra constants, A_1^2 and A_2^2, must be determined. Eq. (26) consequently has four rows instead of two during the analysis of the outer layer.

Table 2 Material properties

Longitudinal modulus, E_1 (MPa)	40887
Transverse modulus, $E_2 = E_3$ (MPa)	7905
Shear modulus, $G_{12} = G_{13}$ (MPa)	2437
Shear modulus, G_{23} (MPa)	2855
Poissons ratio, $\nu_{12} = \nu_{13}$	0.298
Poissons ratio, ν_{23}	0.384

The calculated residual axial, σ_x, and hoop, σ_θ, stresses are shown in Fig. 11. Results using the present technique are compared against those obtained from FEA since no alternative exists. It is clear that the two analysis methods are in excellent agreement. It is interesting that the stress distributions are discontinuous at the interface of the two plies. Even though the apparent stiffnesses of the two plies in the axial and hoop directions are identical, the coupling terms associated with shear result in different stresses for the same strains.
The corresponding radial, σ_r and in-plane shear, $\tau_{x\theta}$ stress distributions are illustrated in Fig. 12. As anticipated, the radial stress is continuous from ply to ply, a requirement of the

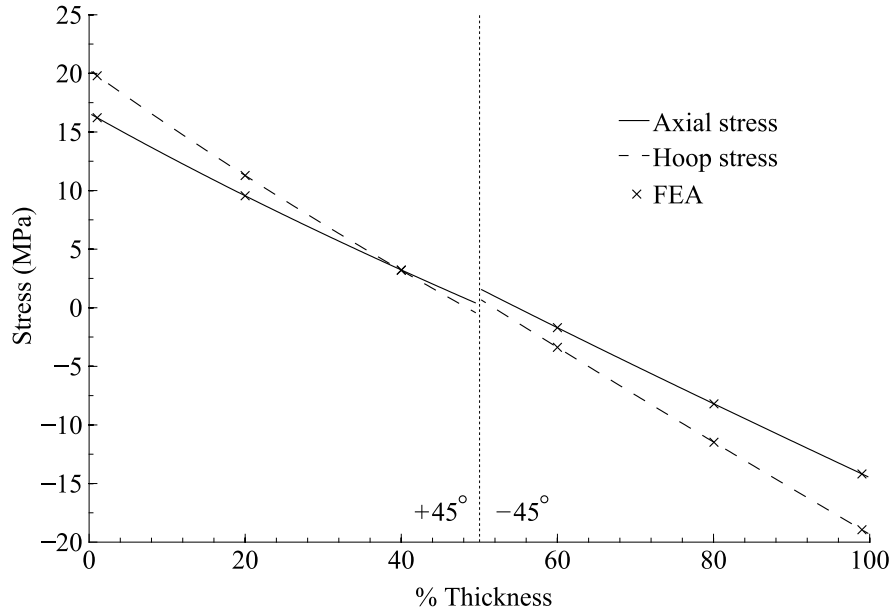

Fig. 11 Axial and hoop residual stresses for $+45°/-45°$ anisotropic pipe, $t/d_i = 0.1875$

boundary conditions. The in-plane shear stress is, however, discontinuous at the ply interface as expected within a layered anisotropic material. The discontinuity is not symmetrically located relative to the line of zero shear stress. This situation arises because coupling between the in-plane shear stress and the axial and hoop strains acts in the opposite sense in each ply.

4 Conclusions

A method of residual stress measurement in layered anisotropic pipes has been presented. This method takes full account of the three-dimensional stress state that exists throughout the wall thickness. The method has been shown to have a system of self-correction, where measurement errors do not propagate through the solution, but only affect the results in the region of error. In addition, the calculated residual stress distributions inherently satisfy the requirement of self-equilibrium. The present method shows excellent agreement with the methods of Sachs [12] and Voyiadjis et al. [25] for a thick-walled isotropic pipe. The present method also correlates very closely with that of the method of Voyiadjis et al. [25] for thin-walled orthotropic pipes. Results from FEA and the present method indicate that the method of Voyiadjis et al. [25] is less accurate for thick orthotropic pipes. The ability of the present method to calculate the residual stress distribution in layered anisotropic pipes has been shown using a moderately thick-walled pipe built up of $+45°$ and $-45°$ plies. The method can be applied to any wall thickness and can be used for isotropic, orthotropic or anisotropic pipes, whether layered or not.

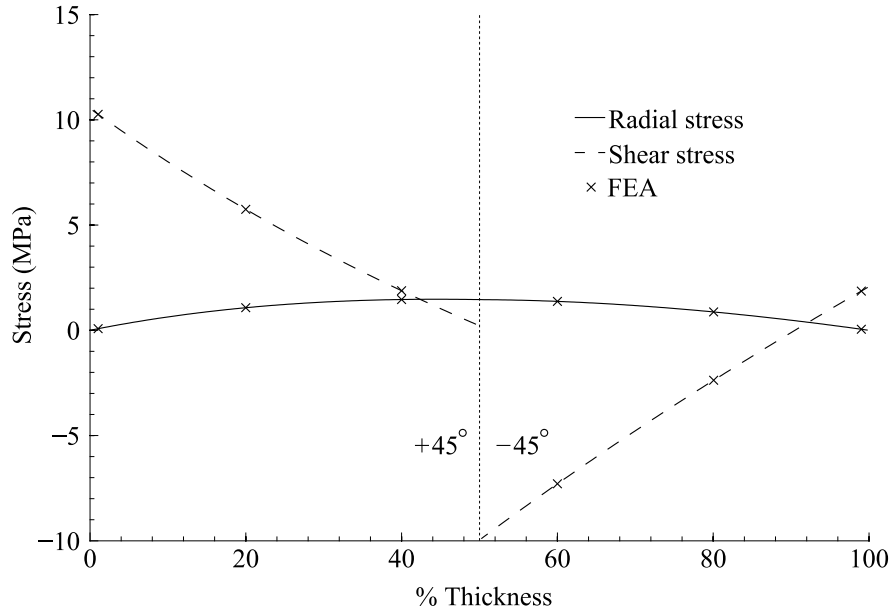

Fig. 12 Radial and shear residual stresses for $+45°/-45°$ anisotropic pipe, $t/d_i = 0.1875$

Acknowledgements

The support of the DST/NRF Centre of Excellence in Strong Materials (CoE-SM) towards this research is hereby acknowledged. Opinions expressed and conclusions arrived at, are those of the authors and are not necessarily to be attributed to the CoE-SM.

References

1. L. L. Meisner, A. I. Lotkov, M. G. Ostapenko, and E. Y. Gudimova. X-ray diffraction study of residual elastic stress and microstructure of near-surface layers in nickel-titanium alloy irradiated with low-energy high-current electron beams. *Applied Surface Science*, 280:398–404, 2013.
2. R. D. Haigh, M. T. Hutchings, J. A. James, S. Ganguly, R. Mizuno, K. Ogawa, S. Okido, A. M. Paradowska, and M. E. Fitzpatrick. Neutron diffraction residual stress measurements on girth-welded 304 stainless steel pipes with weld metal deposited up to half and full pipe wall thickness. *International Journal of Pressure Vessels and Piping*, 101:1–11, 2013.
3. M. B. Prime. Residual stress measurement by successive extension of a slot: The crack compliance method. *Applied Mechanics Reviews*, 52(2):75–96, 1999.
4. H. Gong, Y. Wu, and K. Liao. Research on residual stress measurement technology of aluminum alloy plate based on modified layer removal method. In *1st International Conference on Information Science and Engineering, ICISE*, pages 3839–3842, 2009.
5. F. Yang, Y. Wang, and J. Jiang. Residual stress profile in high carbon rods measured by layer removal technique. *Cailiao Kexue yu Gongyi/Material Science and Technology*, 18(4):579–583, 2010.
6. M. B. Prime. Measuring residual stress and the resulting stress intensity factor in compact tension specimens. *Fatigue and Fracture of Engineering Materials and Structures*, 22(3):195–204, 1999.
7. M. B. Prime and M. R. Hill. Measurement of fiber-scale residual stress variation in a metal-matrix composite. *Journal of Composite Materials*, 38(23):2079–2095, 2004.
8. A. T. DeWald and M. R. Hill. Measurement of bulk residual stress distributions in thick-section components using the contour method. In *Conference Proceedings of the Society for Experimental Mechanics Series*, volume 8, pages 29–31, 2011.

9. P. Pagliaro, M. B. Prime, H. Swenson, and B. Zuccarello. Measuring multiple residual-stress components using the Contour method and multiple cuts. *Experimental Mechanics*, 50(2):187–194, 2010.
10. M. T. Flaman and B. H. Manning. Determination of residual-stress variation with depth by the hole-drilling method. *Experimental Mechanics*, 25(3):205–207, 1985.
11. O. Sicot, X. L. Gong, A. Cherouat, and J. Lu. Influence of experimental parameters on determination of residual stress using the incremental hole-drilling method. *Composites Science and Technology*, 64(2):171–180, 2004.
12. G. Sachs. The Determination of Residual Stresses in Rods and Tubes. *Zeitschrift für Metallkinde*, 19:352–357, 1927.
13. A. Stacey and G. A. Webster. Determination of residual stress distributions in autofrettaged tubing. *International Journal of Pressure Vessels and Piping*, 31(3):205–220, 1988.
14. M. M. Shokrieh, S. Akbari, and A. Daneshvar. A comparison between the slitting method and the classical lamination theory in determination of macro-residual stresses in laminated composites. *Composite Structures*, 96:708–715, 2013.
15. N. Ersoy and O. Vardar. Measurement of residual stresses in layered composites by compliance method. *Journal of Composite Materials*, 34(7):575–598, 2000.
16. M. G. Bateman, O. H. Miller, T. J. Palmer, C. E. P. Breen, E. J. Kingston, D. J. Smith, and M. J. Pavier. Measurement of residual stress in thick section composite laminates using the deep-hole method. *International Journal of Mechanical Sciences*, 47(11):1718–1739, 2005.
17. M. A. Seif and S. R. Short. Determination of residual stresses in thin-walled composite cylinders. *Experimental Techniques*, 26(2):43–46, 2002.
18. M. A. Seif, U. A. Khashaba, and R. Rojas-oviedo. Residual stress measurements in CFRE and GFRE composite missile shells. *Composite Structures*, 79(2):261–269, 2007.
19. J. W. Kim and D. G. Lee. Measurement of residual stresses in thick composite cylinders by the radial-cut-cylinder-bending method. *Composite Structures*, 77(4):444–456, 2007.
20. S. Akbari, F. Taheri-Behrooz, and M. M. Shokrieh. Slitting Measurement of Residual Hoop Stresses Through the Wall-Thickness of a Filament Wound Composite Ring. *Experimental Mechanics*, pages 1–10, 2013.
21. J. Chen, T. Terasaki, T. Akiyama, and K. Kishitake. New concept of equivalent inherent strain for measuring axisymmetric residual stresses. *Journal of Manufacturing Science and Engineering, Transactions of the ASME*, 122(2):304–309, 2000.
22. B. M. Botros. Residual stresses in cold ironed tubes. *International Journal of Mechanical Sciences*, 2(3):195–205, 1960.
23. D. R. Mack. Measurement of residual stress in disks from turbine-rotor forgings - Investigation reveals that both the sachs turning-down method and the concentric-ring method provide reliable measurements of tangential residual stress in a steel disk at the bore hole. *Experimental Mechanics*, 2(5):155–158, 1962.
24. W. A. Olson and C. W. Bert. Analysis of residual stresses in bars and tubes of cylindrically orthotropic materials - Paper presents equations for calculating residual stresses from surface-strain data measured after successive borings in a bar or tube made of a cylindrically orthotropic material. *Experimental Mechanics*, 6(9):451–457, 1966.
25. G. Z. Voyiadjis, P. D. Kiousis, and C. S. Hartley. Analysis of residual stresses in cylindrically anisotropic materials. *Experimental Mechanics*, 25(2):145–147, 1985.
26. G. Z. Voyiadjis and C. S. Hartley. Residual-stress determination of concentric layers of cylindrically orthotropic materials. *Experimental Mechanics*, 27(3):290–297, 1987.
27. J. Rasty, X. Le, M. Baydogan, and J. F. Cárdenas-García. Measurement of residual stresses in nuclear-grade Zircaloy-4(R) tubes - Effect of heat treatment. *Experimental Mechanics*, 47(2):185–199, 2007.
28. S. G. Lekhnitskii. *Anisotropic plates, 2nd edn*. Gordon and Breach, 1968.
29. C. T. Herakovich. *Mechanics of Fibrous Composites*. John Wiley & Sons, Inc., 1998.
30. S. G. Lekhniitski. *Theory of Elasticity of an Anisotropic Elastic Body*. Holden-Day, Inc., San Francisco, 1963.
31. R. E. Scherrer. Filament-Wound Cylinders with Axial-Symmetric Loads. *Journal of Composite Materials*, 1:344–355, 1967.
32. E. Reissner. On axially uniform stress and strain in axially homogeneous cylindrical shells. *International Journal of Solids and Structures*, 6(1):133–138, 1970.
33. N. J. Pagano. Stress Gradients in Laminated Composite Cylinders. *Journal of Composite Materials*, 5:257–265, 1971.
34. E. Reissner and W. T. Tsai. Pure Bending, Stretching, and Twisting of Anisotropic Cylindrical Shells. *Journal of Applied Mechanics*, 4:168–174, 1974.
35. G. Orgill and J. F. Wilson. Finite Deformations of Nonlinear, Orthotropic Cylindrical Shells. *Journal of Applied Mechanics, Transactions ASME*, 53(2):257–265, 1986.